Miocene to Pleistocene Palaeoceanography of the Andaman Region: Evolution of the Indian Monsoon on a Warmer-Than-Present Earth

Wolfgang Kuhnt, Ann E. Holbourn, Janika Jöhnck and Julia Lübbers

Abstract The Andaman Sea is ideally situated to assess the sensitivity of the Indian Monsoon to insolation forcing and to changes in climate boundary conditions such as global ice volume and greenhouse gas concentrations on a warmer-than-present Earth. Sediment archives from this region record the monsoonal discharge of water and sediment from mountainous areas at the southern slope of the Eastern Himalayas, the western slopes of the Arakan Mountains and Indo-Burman Ranges and from the catchment of the Irrawaddy, Sittang and Salween Rivers. New sediment cores recovered during International Ocean Discovery Program (IODP) Expedition 353 (iMonsoon) provide the first complete millennial-scale resolution record of the Indian Monsoon over the late Neogene, when major changes in the Indian and East-Asian monsoonal subsystems occurred. Initial results from sediment natural gamma ray core-logging and foraminiferal stable isotope analyses indicate that a long-term increase in physical weathering and erosion coincided with a prolonged late Miocene cooling trend between ~7 and 5.5 Ma. Monsoonal erosion remained intense during the subsequent warming episode between 5.5 and 5.3 Ma, probably associated with a northward shift of the monsoonal rain belt. Ocean mixed layer oxygen isotope records indicate freshening of the Andaman Sea during late Miocene warm isotope stages as during Pleistocene interglacials. Knowledge of this past evolution of freshwater and sediment discharge from one of the core areas of Indian Monsoon precipitation is essential to better predict trends and consequences of monsoonal spatial variability with future climate change.

Keywords International Ocean Discovery Program · Miocene · Palaeoceanography · Indian monsoon · Andaman Sea

W. Kuhnt (✉) · A. E. Holbourn · J. Jöhnck · J. Lübbers
Institute of Geosciences, Christian-Albrechts-University, Kiel, Germany
e-mail: Wolfgang.Kuhnt@ifg.uni-kiel.de

J. S. Ray and M. Radhakrishna (eds.), *The Andaman Islands and Adjoining Offshore: Geology, Tectonics and Palaeoclimate*, Society of Earth Scientists Series,
https://doi.org/10.1007/978-3-030-39843-9_13

1 Introduction

Despite half a century of intense research, the physical forcing processes that drive the long-term variability of monsoonal precipitation within the Earth's strongest hydrological regime are still a matter of vigorous debate. These controversies largely stem from the fact that the Indo-Asian Monsoon consists of a series of regional monsoonal subsystems (Arabian Sea Monsoon, Indian Monsoon, East Asian Monsoon, Australian Monsoon), which exhibit differing intensity, temporal variability and sensitivity to driving mechanisms. The extent to which these subsystems are driven by an underlying single, large-scale, physical process has recently been the focus of discussions related to the evolving concept of a "global monsoon" (Wang and Ding 2008; An et al. 2015; Wang et al. 2017). These differing views largely stem from seasonal and regional differences in the manifestation of the monsoon (e.g., heavy rain over parts of the Indian subcontinent and the Bay of Bengal versus strong winds over the western Arabian Sea and parts of the open Indian Ocean) and from different assessments of the relative importance of external (orbital insolation) versus internal (boundary conditions such as ice volume, atmospheric greenhouse gases and topography) forcing factors for regional monsoon subsystems (e.g., Ruddiman 2006; Clemens and Prell 2007). Monsoonal records extending over orbital to tectonic timescales, in particular over warmer intervals of Earth's climate history characterized by fundamentally different internal boundary conditions, are crucial to evaluate the role of internal forcing factors in controlling the evolution of the monsoon.

To date, only a handful of records, generally at relatively low-resolution, retrace the deep time evolution of the Indian Monsoon. Micropalaeontological data from the Arabian Sea and from the central East Asian continent initially suggested that the intensity of monsoonal winds increased substantially at ~8–7 Ma (Kroon et al. 1991; Prell et al. 1992; Prell and Kutzbach 1997; An et al. 2001). The coeval emergence and expansion of arid-adapted C4 floras in South and Central Asia, indicative of reduced precipitation or decreased atmospheric CO_2 concentrations (e.g., Quade and Cerling 1995; Cerling et al. 1997; Huang et al. 2007), were also linked to an intensification of the dry boreal winter monsoon over the Asian continent. These changes were associated with concurrent changes in the erosional regime and tectonic evolution of the Himalayas and Tibetan Plateau during the late Miocene-Pliocene (Molnar et al. 1993, 2010; Molnar 2005). However, in contrast to the widely-held view of a late Miocene intensification of the Indo-Asian Monsoon, a much earlier onset of the monsoon has also been proposed, based on changes in Central Asian climate, weathering regime and related sediment fluxes (Guo et al. 2002; Sun and Wang 2005; Clift et al. 2008).

The mainstream view of a direct linkage between the uplift and expansion of the Tibetan Plateau, the intensification of the Indo-Asian Monsoon, global cooling and atmospheric pCO_2 decline has been challenged in recent years by new observations and refined palaeoclimate models (see discussion in Qiu 2013). For example, Rodriguez et al. (2014) suggested that the ~8–7 Ma intensification of monsoonal

winds in the Arabian Sea, inferred on the basis of increased abundances of *Globigerina bulloides*, was an artifact of enhanced preservation related to uplift of the Owen Ridge and that the importance of the uplift of the Tibetan plateau was substantially overestimated in early climate models (Boos and Kuang 2010; Molnar et al. 2010; Liu and Yin 2011; Molnar and Rajagopalan 2012). In particular, the "classic" argument, that the rise of the Tibetan plateau near 10 Ma led to strengthening of the Indo-Asian Monsoon (Harrison et al. 1992; Molnar et al. 1993; Prell et al. 1992; Prell and Kutzbach 1997) has ben challenged by more recent studies, associating a higher eastern Tibet with decreasing rainfall over NW India between 10 and 7 Ma (Molnar and Rajagopalan 2012). A fundamental shortcoming in the debate on the late Miocene-Pliocene onset or intensification of the monsoon versus longer-term perspectives of variability is the lack of records from the core area of the Indian Monsoon in the Bay of Bengal. Well-dated proxy records of precipitation, salinity, terrigenous runoff and productivity from the Bay of Bengal and Andaman Sea are essential to monitor the intensification of the Indian Monsoon in its core region, where increased rainfall, and not strengthened wind, characterizes the monsoon.

IODP Expedition 353 (iMonsoon) targeted the monsoonal precipitation signal in its core geographic region of influence, including the western margin of the Andaman Sea and investigated long-term monsoonal circulation changes through the drilling of high-resolution sedimentary archives. The Bay of Bengal and Andaman Sea presently receive one of the largest freshwater and sediment discharges in the world from three major river systems that are primarily influenced by the Indian Monsoon. This region is, therefore, ideally located to monitor past monsoonal trends in relation to changes in insolation forcing and in climate boundary conditions such as orography, global ice volume and greenhouse gas concentrations. Two sites (U1447, 10° 47.40′ N/93° 00′ E, 1391 m water depth and U1448, 10° 38.03′ N/93° 00′ E, 1098 m water depth) in the vicinity of the Andaman Islands recovered extended upper Miocne to Pliocene successions, which provide an outstanding opportunity to assess the sensitivity of the Indian Monsoon to internal and external forcings on a warmer-than-present Earth. Here, (1) we integrate new isotope data from Sites U1447 and U1448 with proxy runoff data to track the evolution of the Indian Monsoon over the late Miocene to earliest Pliocene, an interval marked by important reversals in cooling and warming trends, and (2) we compare monsoonal trends on a Pleistocene bipolar glaciated world over the last million years to monsoonal variability on a warmer Earth in the late Miocene.

2 Neogene Sedimentary Archives of the Andaman Region: A Key to Reconstruct the Indian Palaeomonsoon

The Andaman Island arc system results from the oblique subduction of the Indo-Australian plate beneath the Eurasian plate. Subsequent stretching and rifting of the overriding plate since the early Miocene led to formation of an active spreading center

in the deepest portion of the Andaman Sea during the late Miocene-early Pliocene (Raju et al. 2004; Curray 2005; Singh et al. 2013; Morley 2016). An accretionary wedge complex formed in the west of the spreading center, consisting of a series of shallower basins bordered by back thrust faults within the accretionary wedge. Garzanti et al. (2013) argued for distinctly different source areas for the Andaman flysch on the western side of the Andaman Islands. These authors suggested that it was associated with the Bengal Fan and consisted of re-deposited material from the Oligocene Irrawaddy deep sea fan (Allen et al. 2008) that was offscraped in the rear of the accretionary prism. In contrast, the terrigenous sediment input to the eastern margin of the Andaman Islands originates directly from river discharge from the Indo-Burman mountain ranges and the Irrawaddy-Salween river system and did not change since the early Miocene.

IODP Expedition 353 Sites U1447 and U1448 targeted the Nicobar-Andaman Basin between the Diligent and Eastern Margin faults, which provided a unique opportunity to recover undisturbed sedimentary successions in intermediate water depths deposited well above the calcite lysocline. Site U1447 is located at 10° 47.40′ N/93° 00′ E in 1391 m water depth, ~45 km east of Little Andaman Island, within a small basin on the eastern flank of a rise separating north-south oriented basins associated with the Eastern Margin and Diligent fault zones. Seismic profiles indicate that ~740 m of sediments overlay the accretionary wedge complex at this location (Fig. 1). The main drilling objective at this site was to recover Miocene to Holocene sediments in order to reconstruct changes in sea surface salinity and runoff associated

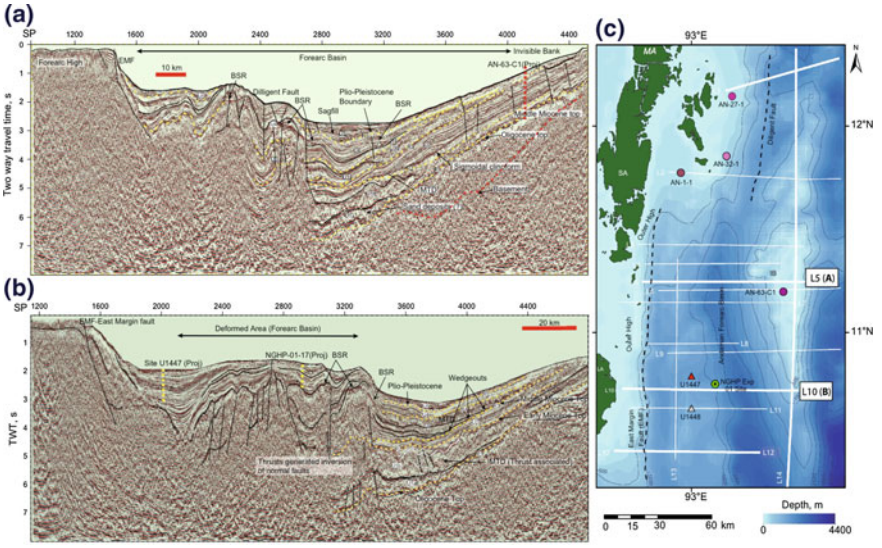

Fig. 1 Seismic stratigraphy of the eastern margin of the Andaman Ridge (from Pandey et al. 2017), under Creative Commons Attribution 4.0 International License (http://creativecommons.org/licenses/by/4.0/). E-W seismic line L5 at ~11° 45′N (**a**), E-W seismic line L10 at ~10° 45′N (**b**), Position of seismic lines on the satellite bathymetry map after Sandwell and Smith (2009) (**c**)

with local summer monsoon rainfall within the catchments of the Irrawaddy and Salween Rivers at tectonic to suborbital timescales. Site U1448 is located at 10° 38.03′ N/93° 00′ E in 1098 m water depth, ~44 km east of Little Andaman Island on a rise to the west of the deeper Site U1447. Seismic profiles indicate that ~420 m of sediments overlay the accretionary wedge complex at this location (Fig. 1). Site U1448 was selected due to its elevated position, protecting it from the influence of turbidites, which affect sedimentation through the Pliocene and lower Pleistocene at Site U1447.

Today, the terrigenous input to this part of the Andaman Sea stems dominantly from the Irrawaddy and Salween Rivers (Colin et al. 1999; Ali et al. 2015). Recent provenance studies using clay minerals and Sr- and Nd-isotopes indicate that this main sediment source has not fundamentally changed since the late Miocene (France-Lanord et al. 1993; Cawthern et al. 2014; Phillips et al. 2014). The variability in the amount and composition of this terrigenous discharge is linked to monsoon intensity in the source area through erosion, chemical weathering and transport at millennial, orbital and tectonic timescales. Calibration studies of core top sediments have shown that different elemental ratios can reliably trace different weathering regimes and that ratios of mobile versus immobile elements track the intensity of chemical weathering and/or erosion in the source areas on orbital and suborbital timescales (Liu et al. 2008; Wan et al. 2007, 2009). The Andaman Sea, thus, offers a unique opportunity to monitor changes in monsoon strength, weathering rates and transport of particulate materials to the ocean, in particular over the critical late Miocene to Pliocene interval, when major re-organizations of monsoonal patterns are documented in other monsoonal regions (e.g., Clift and Plumb 2008; Holbourn et al. 2018).

3 Modern (Late Pleistocene to Recent) Oceanographic and Climatic Setting

3.1 The Andaman Area and SE Asian Margin of Burma: A Core Area of Indian Monsoon Precipitation

The Andaman Sea is influenced by three major river systems, which give rise to one of the largest freshwater and sediment discharges in the world. The Ganges-Brahmaputra River system is ranked fourth among the world's rivers as a source of freshwater to the oceans (1120 km^3/yr) and supplies more sediment to the ocean than any other river in the world (1060 Mt/yr) (Milliman and Farnsworth 2011). The Irrawaddy and Salween Rivers together discharge up to 640 km^3/yr of freshwater and deliver up to 540 Mt/yr sediment (Figs. 2 and 3) (Milliman and Farnsworth 2011). The discharge of water and sediment to the Andaman Sea mainly originates from mountainous areas at the southern slope of the Eastern Himalayas (northern part of

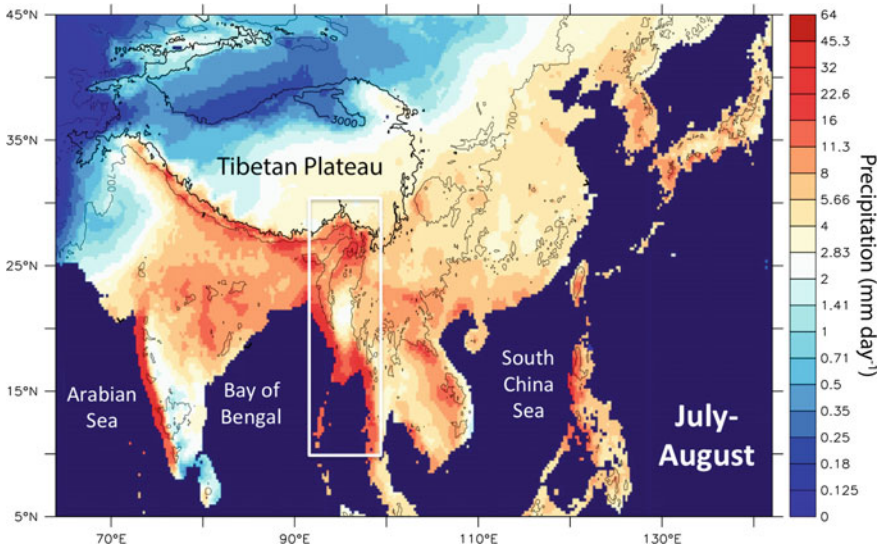

Fig. 2 Indian Summer Monsoon precipitation along the northeast margin of the Indian Ocean (July–August mean precipitation from APHRODITE (mm/day 1951–2007 modified after Day et al. 2015)). The white rectangle indicates the drainage area for runoff to the Andaman Sea

the Irrawaddy catchment), the western slopes of the Arakan Mountains and Indo-Burman Ranges and from the catchment of the Salween and Sittang Rivers, where orography creates one of the most important precipitation domains of the Indian Monsoon (Fig. 2) (Day et al. 2015).

During the last glacial cycle, sediment discharge from freshly eroded sources increased during intervals of Northern Hemisphere cooling such as the Younger Dryas (YD), Last Glacial Maximum (LGM) and Heinrich stadials of Marine Isotope Stage (MIS) 3 (Awasthi et al. 2014). Awasthi et al. (2014) suggested that this change in sediment provenance was linked to a southward shift of the main summer monsoon precipitation belt from the Himalayas during Northern Hemisphere cooling, without any major reduction in monsoon intensity. An alternate hypothesis is that enhanced physical erosion induced by a cooler and dryer climate and intensified glacial erosion in the highland of the Irrawaddy River may have produced larger volumes of unaltered sediment (Colin et al. 2006). The lower glacial sea level additionally increased the transport efficiency of rivers in the lower part of their catchment, thus contributing to increased discharge of freshly eroded unaltered sediment from the Himalayas into the Andaman Sea.

Over the last 280 kyr, clay mineralogy and chemical weathering proxy records in the deep central Andaman Sea were characterized by prominent 23 kyr periodicity (Colin et al. 1999; Cao et al. 2015), which is in phase with the Northern Hemisphere insolation driven climate in the lower Indo-Burman ranges and Irrawaddy River plain. Strong chemical weathering in the Irrawaddy plain must have dominated the terrigenous discharge during periods of intensified monsoon precipitation

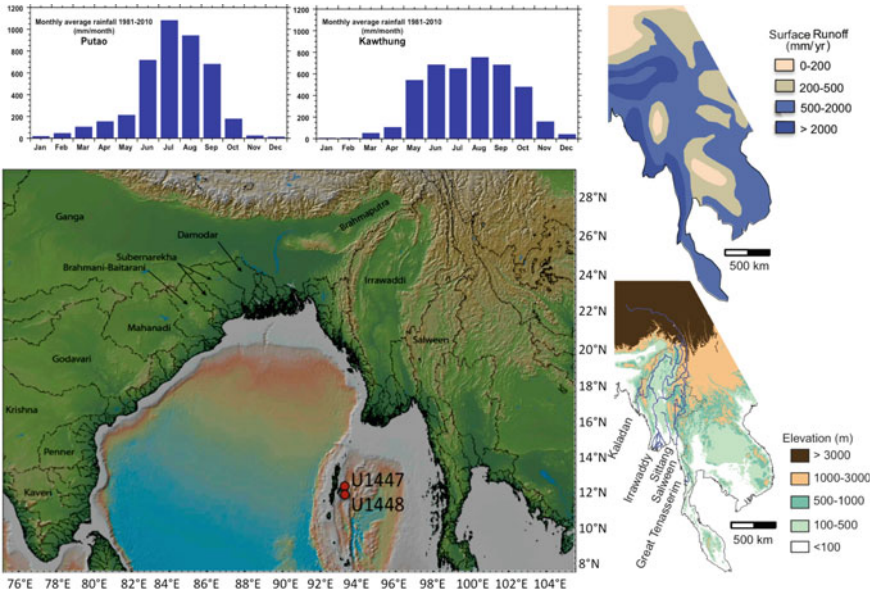

Fig. 3 Seasonal precipitation and runoff patterns of the Irrawaddy and Salween Rivers and location of IODP Sites U1447 and U1448 in relation to the main drainage basins on the Asian continent. Today, sediment and freshwater runoff at Sites U1447 and U1448 originates mainly from the Irrawaddy and Salween drainage basins on the Asian continent. Average monthly rainfall at Putao in Northern Myanmar and Kawthung at the southern end of Myanmar for the years 1981–2010 are from Aung et al. (2017). The extent, elevation and annual surface runoff of drainage basins are redrawn and simplified after Milliman and Farnsworth (2011)

in the lower Burman Ranges relative to input from the high Burman ranges, where physical erosion dominates. The northern Andaman Sea is characterized by unusually high suspended sediment concentrations due to high and seasonal sediment discharge from the Irrawaddy, Sittang and Salween Rivers and intense resuspension of sediments by strong tidal currents. This suspended sediment load is dispersed into the deep Andaman Sea as a mid-water nepheloid layer, which acts as the main source of sediment supply to the deep Andaman Sea (Ramaswamy et al. 2004). Sediment dispersed from the Bengal shelf and western and southern margins of Myanmar by intensified westerly surface currents during the winter season provides a supplementary source of terrigenous input from the Indo-Burman ranges into the Andaman Sea (Fig. 4). This input was already active during the LGM and increased in intensity during the last deglaciation (Awasthi et al. 2014). This direct coupling between monsoonal erosion and transport from a major hotspot of summer monsoonal precipitation in the Himalayan and Indo-Burman mountain ranges with its discharge into the sediment sink makes the Andaman Sea a prime area for monitoring the variability of the Indian Monsoon on suborbital, orbital and tectonic timescales.

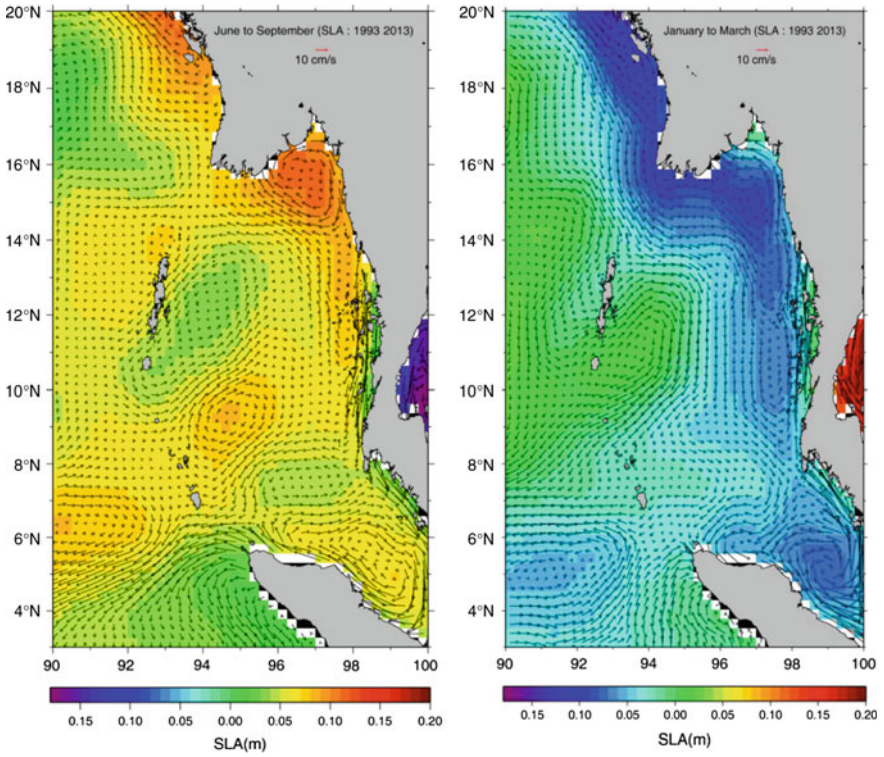

Fig. 4 Surface circulation in the Andaman Sea during summer (left) and winter (right) obtained by deriving geostrophic currents based on monthly mean climatology of sea level anomaly during the period 1993–2013 from BOBLME 2015 (Brewer et al. 2015). Note the important inflow of cool, low-salinity waters from the Bay of Bengal through the northern passage into the Andaman Sea and the outflow from the Andaman Sea through the middle passage into the southern Bay of Bengal during winter. In contrast, during the boreal summer months dominates the outflow of Andaman Sea water through the southern Great Channel into the equatorial Indian Ocean

3.2 Circulation and Water Mass Properties in the Andaman Sea

The Andaman Sea is connected by a broad passage at 6° N (Great Channel) to the open equatorial Indian Ocean and by two main passages at 10° N (Ten Degree Channel) and 15° N (Preparis Channel) to the Bay of Bengal (Fig. 4). Circulation through these passages affects the dynamic interaction between near-surface water masses of the eastern equatorial Indian Ocean and the Bay of Bengal (Chatterjee et al. 2017). Whereas the mean coastal circulation within the Andaman Sea and around the Andaman and Nicobar Islands is strongly influenced by remote atmospheric forcing from the equator, the seasonally changing current directions and intensities (Figs. 4 and 5) are to a large extent driven by local winds (Chatterjee et al. 2017).

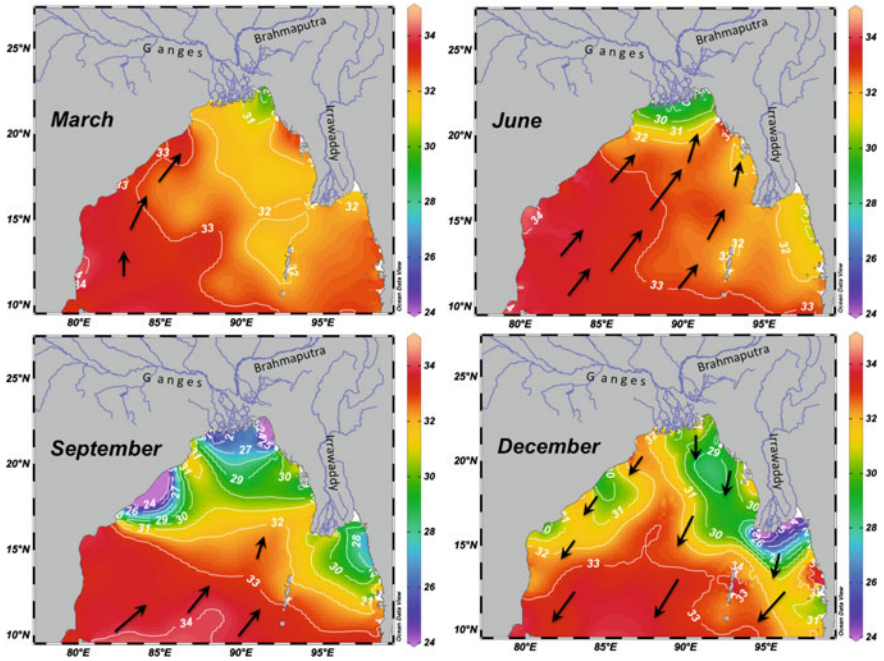

Fig. 5 Bay of Bengal and Andaman Sea salinity in September and December based on WOA 2013 data (Talley 2013) and simplified prevailing wind forcing based on Hastenrath and Lamb (1979) and Varkey et al. (1996)

Sea surface temperature and salinity in the Andaman Sea are largely controlled by the marked seasonality in monsoonal wind, precipitation and runoff induced by the switch between wet southwest (boreal summer) monsoon and dry northeast (boreal winter) monsoon (Fig. 5) (Varkey et al. 1996). Lowest salinities (~32 Practical Salinity Units (PSU)) in the Andaman Sea occur during peak monsoon runoff from smaller southern Myanmar rivers in September.

Surface salinity and ocean currents in the equatorial northeastern Indian Ocean also reflect the seasonal wind forcing by the southwest monsoon and the northeast monsoon (Schott et al. 2009). This monsoon driven circulation is characterized by a marked seasonal contrast between dominant freshwater export from the Bay of Bengal and northern Andaman Sea during boreal winter and eastward transfer of saline and nutrient-rich waters from the Arabian Sea during boreal summer (Fig. 5) (Gordon et al. 2016; Goswami et al. 2016). The influx of nutrient-rich, high-salinity water originating from a vigorous westerly current (Southwest Monsoon Current) that carries high-salinity waters eastward around the tip of India into the southern Bay of Bengal is reflected in the regional salinity and productivity patterns during July, August, and September (Fig. 5). Only the uppermost 100 m of the tropical eastern Indian Ocean in the Bay of Bengal and Andaman Sea consist of a low-salinity water mass derived from river runoff from India and Indochina with surface salinity

strongly fluctuating seasonally, but remaining below 33.0 PSU throughout the year. The southward extension of this low-salinity surface water mass is highest during October–December, when it reaches as far southeast as the Andaman archipelago and is lowest during April–June (Fig. 5).

The transfer of nutrient-rich surface waters originating from the upwelling systems at the eastern margins of the Arabian Sea during the boreal summer monsoon impacts productivity as well as the amount and composition of particle fluxes to the deep sea in the southern Bay of Bengal and Andaman Sea (Unger et al. 2003; Unger and Jennerjahn 2009). The ratio of particulate deep-ocean organic matter flux to primary productivity is unusually high in the Bay of Bengal (Ittekkot et al. 1991; Lutz et al. 2002; Gauns et al. 2005). This has been explained by high fluxes of riverine mineral particles, to which sinking organic matter can aggregate to, resulting in increased sinking speed and reduced decomposition rates of organic matter in the water column and at the sediment surface (Klaas and Archer 2002; Iversen and Ploug 2010; Le Moigne et al. 2013). This high abundance of mineral ballast in the present-day Bay of Bengal influences not only the rate and depth of organic matter remineralization, and thus the efficiency of export of organic matter to the seafloor (Kwon et al. 2009), but also contributes to the development of a weaker and more contracted oxygen minimum zone (OMZ) than in the Arabian Sea (Al Azhar et al. 2017).

The bottom water at the margins of the Andaman Islands is occupied by a mixture of Indian Deep Water (IDW) originating from the equatorial Indian Ocean and local thermocline water. Two water masses occupy the thermocline of the tropical Indian Ocean in the Bay of Bengal and Andaman Sea, Indian Central Water (ICW), originating from the Southern Hemisphere Indian Ocean and Indonesian Throughflow Water (ITW), which is derived from North Pacific Intermediate Water modified by intense mixing during its passage through the Indonesian archipelago. The oxygen content of these intermediate water masses becomes strongly reduced during their transfer into the Bay of Bengal and Andaman Sea and the admixing of ITW results in some freshening of the ICW along its path into the Bay of Bengal. However, the low oxygen levels indicate an extremely low renewal rate for the thermocline waters of the Bay of Bengal (Tomczak and Godfrey 2005). Intermediate waters in the Andaman Sea are strongly influenced by the OMZ in the Bay of Bengal resulting in concentrations of dissolved oxygen below 50 μmol/kg and $\delta^{13}C$ values below zero (Fig. 6) (Talley 2013).

Analysis of Andaman Sea surface sediments show that planktic foraminifers are abundant and well preserved in water depth above ~1800 m (>100,000 individuals/gram) and decrease to <100 individuals/gram in water depth below 3000 m (Frerichs 1971), indicating that the foraminiferal lysocline hovers close to 3000 m. Pteropod preservation profiles in sediments off Middle Andaman Island indicate a sharp decline of pteropods between 1108 and 1147 m water depth, while planktonic foraminifers remain abundant and well-preserved (Bhattachjarjee 2005). These sediment surface distribution data also indicate a deepening of the aragonite compensation depth from the northern Andaman Sea to the south, suggesting that reduced carbonate production and carbonate ion concentration and the resulting shallowing

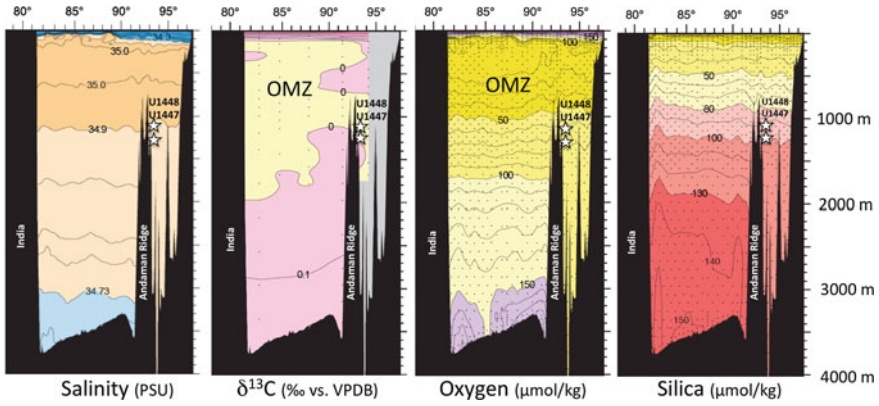

Fig. 6 Bay of Bengal and Andaman Sea salinity, $\delta^{13}C$, oxygen and silicate profiles along WOCE section I01 at 9° N (Talley 2013). Note the increasingly fresh, $\delta^{13}C$ and oxygen-enriched surface waters towards the Andaman Sea

of the aragonite compensation depth in the northernmost Andaman Sea are related to the freshwater discharge of the Irrawaddy River (Bhattachjarjee 2005).

4 Materials and Methods

4.1 Coring and Sampling Strategy

Three holes were drilled at Site U1447, ranging in depth from 24.4 to 738.0 m below seafloor (mbsf). In Hole A, 29 cores were retrieved with the Advanced Piston Corer (APC) down to 261.0 mbsf, with a total core recovery of 268.69 m. Below this interval, the half-length APC system recovered 15 cores down to 67.8 mbsf and 44 cores were cut with the Extended Core Barrel (XCB) system down to 409.2 mbsf. Holes U1447B and U1447C were only drilled with the APC system, down to 24.45 and 161.65 m.

At Site U1448, three holes were drilled down to 420.60 mbsf (U1448A), 358.22 mbsf (U1448B) and 34.71 mbsf (U1448C). Hole A was drilled to 204.32 mbsf with the APC system, then down to 343.60 mbsf with the half-length APC system and to a final depth of 420.60 mbsf with the XCB system. Hole B was drilled down to 177.71 mbsf with the APC system, then to 358.22 mbsf with the half-length APC system. A complete splice consisting of Hole A and B was constructed down to ~345 meters composite depth, whereas the deeper part of the U1448 splice consists of a single hole (U1448A) drilled with the XCB system. Core recovery in this lower part was extremely good (101%) with minimal gaps between cores and complete

recovery of the stratigraphic succession. Postcruise sampling of the upper Miocene and lower Pliocene sediment successions for stable isotope analyses at Sites U1447 and U1448 was carried out in 10 cm intervals, which approximately corresponds to millennial-scale temporal resolution.

4.2 Benthic Foraminiferal Isotopes

Samples of 30 cc volume were oven dried at 40 °C and weighed before washing over a 63 μm sieve. Residues were oven dried at 40 °C on a sheet of filter paper, then weighed and sieved into different size fractions. We measured $\delta^{18}O$ and $\delta^{13}C$ in the epifaunal benthic foraminifers *Cibicidoides wuellerstorfi* and/or *Cibicidoides mundulus*. Well-preserved tests were broken into large fragments, cleaned in ultrapure ethanol in an ultrasonic bath, decanted and again dried at 40 °C. Stable carbon and oxygen isotopes were measured with a Finnigan MAT 253 mass spectrometer at the Leibniz Laboratory, University of Kiel. The instrument is coupled on-line to a Carbo-Kiel Device (Type IV) for automated CO_2 preparation from carbonate samples for isotopic analysis. Samples were reacted by individual acid addition (99% H_3PO_4 at 75 °C). On the basis of the performance of international and lab-internal standard carbonates, the precision is better than ±0.09‰. Paired measurements in Miocene samples from ODP Sites 1146 and 1237 previously indicated no significant offset in $\delta^{18}O$ and $\delta^{13}C$ between *C. wuellerstorfi* and *C. mundulus* (Holbourn et al. 2007, 2018). Results were calibrated using the NIST (National Institute of Standard and Technology, Gaithersburg, Maryland) carbonate isotope standard and NBS (National Bureau of Standard) 19 and NBS 20, and are reported on the Vienna PeeDee Belemnite (VPDB) scale.

5 Neogene Seismic Stratigraphy and Initial Drilling Results from the Andaman Forearc Basin

5.1 Upper Miocene to Pleistocene Sediment Sequence

Sediments recovered at Site U1447 consist of upper Miocene to Pleistocene hemipelagic clays, which include a significant biogenic component as well as thin, fine-grained distal turbidites, primarily composed of redeposited pelagic carbonate material (Clemens et al. 2016). Four distinct lithostratigraphic units were discriminated during Expedition 353. Unit I (0–126.00 m below sea floor (mbsf)) is composed of upper Pleistocene greenish gray clayey nannofossil oozes with foraminifers and of foraminifer-rich nannofossil oozes with clay and only rare occurrences of distal turbidites. Unit II (126.00–329.12 mbsf) consists of upper Pliocene to upper Pleistocene greenish gray foraminifer-rich nannofossil oozes with clay. This unit includes

numerous light gray, foraminifer-rich, calcitic turbidites of varying thicknesses as well as bioclastic-rich layers with authigenic carbonate and foraminifers dominating in the sand or silt size fraction. Unit III (329.12–489.80 mbsf) is composed of upper Miocene to lower Pliocene greenish gray clayey nannofossil oozes to calcareous oozes with glauconite. Unit IV (489.80–740.46 mbsf) consists of upper Miocene greenish gray biosilica-rich clay with varying proportions of glauconite and nannofossils, reaching back to at least 9.83 Ma and with average sedimentation rates of 6 cm/kyr.

Hole U1448A recovered a continuous hemipelagic upper Miocene to Pleistocene succession, which contains all calcareous biostratigraphic markers and is not affected by gravity deposition (turbidites or fine-grained grain flows/debris flows) (Clemens et al. 2016). The upper ~180 m of this succession consist of dark greenish gray clay with varying proportions of nannofossils, foraminifers and biosiliceous microfossils such as sponge spicules and diatoms (Unit I of Pleistocene age). This upper unit is underlain by a ~160 m thick succession of greenish gray clay with nannofossils and foraminifers and extremely low biosilica content (Unit II of earliest Pleistocene to latest Miocene age). The base of this hemipleagic succession consists of ~40 m of dark to light greenish gray clay and nannofossil-rich clay with increased content of siliceous sponge spicules and bioturbation burrows and mottled patches (Unit III of late Miocene age). This lower unit shows distinct variability in lightness related to changes in carbonate content and does not include any turbidites or volcanic ash layers. Consistent sedimentation rates at Site U1448 (5–6 cm/ky) enable high-resolution palaeoclimatic reconstructions using calcareous and organic proxy indicators of palaeotemperature and salinity in a continuous succession reaching back to the late Miocene (~6.2 Ma).

5.2 Middle to Late Miocene Unconformity

Reflector R3 (“Mid-Miocene Top”) is a critical marker in the regional sequence stratigraphic scheme of the western margin of the Andaman Sea (Pandey et al. 2017). This reflector forms the boundary between seismic sequence U3 (basin fill, late Miocene) and the sigmoidally prograding sequence U2 (middle Miocene), which includes mass transport deposits due to the regional uplift of basinal highs (Pandey et al. 2017). These authors correlated Reflector R3 with the major sea level regression at ~11 Ma in the sequence stratigraphic scheme of Haq et al. (1987). However, recent benthic foraminiferal isotope records indicate that a major expansion of the East Antarctic Ice Sheet and an associated sea-level fall of ~50 m occurred at ~13.8 Ma, followed by a further smaller expansion of the cryosphere at ~13.1 Ma (e.g., Holbourn et al. 2005, 2018). We therefore suggest that Reflector R3 represents a combination of regional uplift due to intensified compressive tectonic activity with a major eustatic sea-level fall between 13.9 and 13 Ma.

A major middle to late Miocene unconformity was revealed at 379.11 mbsf (Interval U1448-56X-5, 44–66 cm) during IODP Expedition 353 (Figs. 7 and 8). The

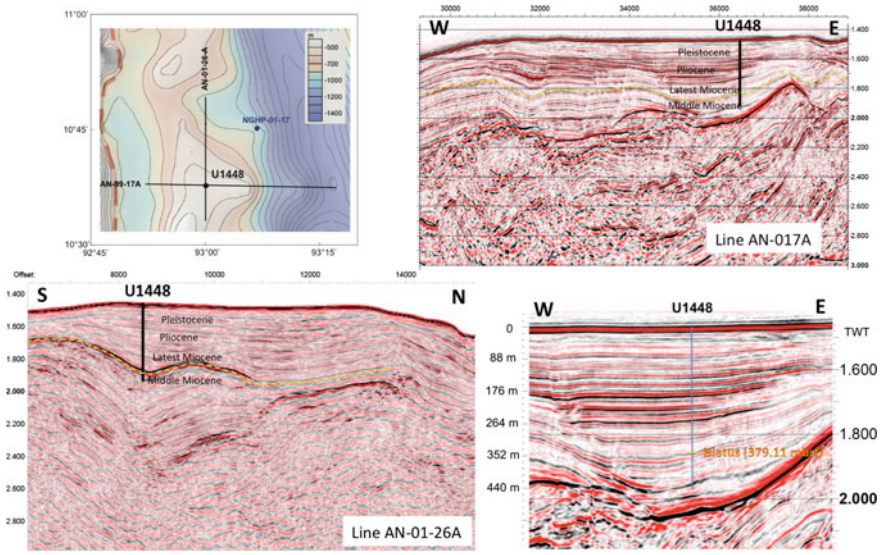

Fig. 7 Seismic expression of middle-late Miocene unconformity and hiatus at IODP Site U1448 from Clemens et al. (2016). Note the lateral N-S and E-W extension and the general northward dip of the unconformity, which may be reflected in the inclined unconformity plane in Hole U1448A

unconformity is expressed as an erosive sedimentary contact representing a major sedimentary hiatus that encompasses the time interval between >5.94 (first biostratigraphic datum above the contact, last occurrence of the calcareous nannoplankton marker *Reticulofenestra rotaria*) and <14.53 Ma (last biostratigraphic datum below the contact, last occurrence of the planktonic foraminifer *Praeorbulina sicana*) (Fig. 9) (Clemens et al. 2016). We suggest that this hiatus is the local expression of Reflector R3, indicating that tectonic changes in the late middle to early late Miocene resulted in regional deformation of the seafloor topography and to a local interruption of deep water sedimentation over periods of several million years at the eastern margin of the Andaman islands (Fig. 7).

Reflector R3 was not reached in Hole U1447A, which was terminated at 738 mbsf, close to the base of the sedimentary succession, dated as 9.83 Ma, on top of the accretionary wedge (Clemens et al. 2016). The earlier onset of pelagic drape sedimentation following the middle-late Miocene unconformity at this deeper site suggests that this unconformity may have formed on top of a northward inclined surface, which developed during a compressional phase in the late middle Miocene. However, sediments within the interval ~6.5 to 6.2 Ma, which corresponds to the onset of deep marine sedimentation at Site U1448 following the Reflector R3 unconformity were not recovered in Hole U1447A due to the loss of Core U1447A-70X. A lithological change, also suggested by a stepped increase in the potassium content of the sediment within this interval, may account for this unexpected loss.

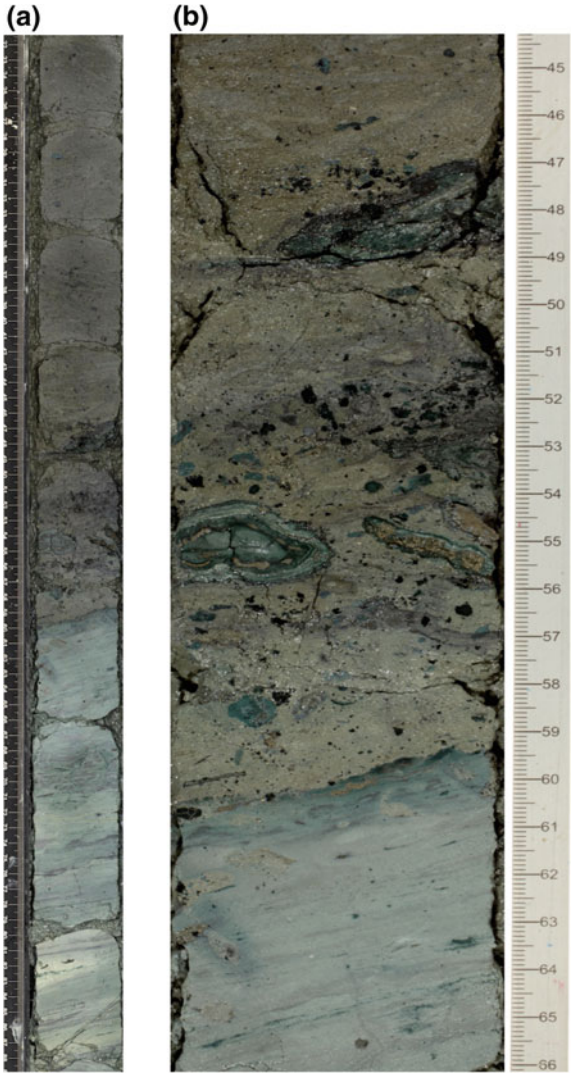

Fig. 8 Middle to late Miocene unconformity in Hole U1448A-56X-5, 44-66 cm (Clemens et al. 2016): sharp contact between nannofossil clay with dark green glauconite and pyrite nodules and underlying clayey biosiliceous ooze (**a**). Burrows in the upper few centimeters of the underlying unit contain nannofossil clay of the overlying unit, indicating the sedimentary nature of the contact (**b**). Nannofossils in the upper unit give a late Miocene age (NN11), whereas the lower unit is of middle Miocene age (NN4)

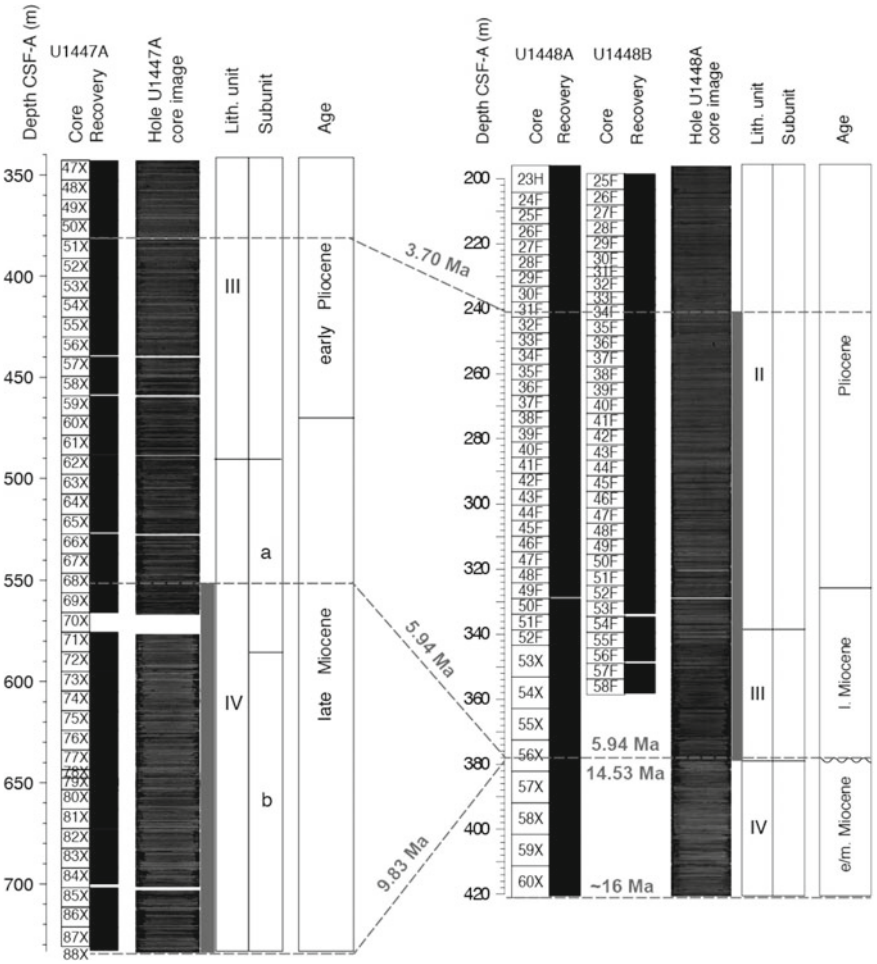

Fig. 9 Correlation of Miocene to lower Pliocene sedimentary successions of Sites U1447 and U1448. Gray bar indicates continuous spliced sequence spanning ~9.9 to 3.7 Ma. Age assignments are based on revised shipboard biostratigraphy of IODP Expedition 353 (Clemens et al. 2016, and Clara Bolton, pers. comm. 16/2/2016)

5.3 Enigmatic Middle Miocene Sediment Sequence

Middle Miocene sediments (seismic unit U2 of Pandey et al. 2017) recovered below the sedimentary hiatus at Site U1448 are composed of light greenish gray bioturbated biosiliceous ooze with varying proportions of clay and nannofossils. Calcium carbonate (between 20 and 30%) and TOC (between 0.2 and 0.4%) concentrations are lower than in the upper Miocene succession (Clemens et al. 2016). Benthic foraminifers are rare, poorly to moderately preserved, mainly consisting of taxa adapted to low

oxygen conditions and enhanced levels of organic matter flux to the sea-floor. Sedimentologic evidence for gravity-driven mass transport deposition of large parts of this sequence includes irregular laminated bedding, microfaults and the presence of small allochthonous mottles and clasts (Clemens et al. 2016).

6 Neogene Evolution of the Indian Monsoon

6.1 Holocene Aridification Linked to Southward Shift of Inter-tropical Convergence Zone?

Most proxy records indicate a decrease in monsoonal precipitation from the Holocene Climate Optimum to the relatively cool pre-industrial late Holocene (Fleitmann et al. 2003; Gupta et al. 2003; Ponton et al. 2012). However, the intensity, spatial variability and causes of the Holocene decrease in wind and precipitation, leading to aridification of large parts of the Indian subcontinent, are still under debate. Southwest Indian records exhibit a long-term increase in summer monsoon rainfall, most probably driven by orographic precipitation in the western Ghats (Sarkar et al. 2000). In contrast, instrumental and proxy records of Holocene monsoonal precipitation over central India revealed increasing interannual variability of summer rainfall with prolonged periods of reduced monsoonal precipitation (monsoon breaks) (Gadgil 2003; Staubwasser and Weiss 2006; Sinha et al. 2011a, b). Speleothem-based precipitation reconstructions suggested that monsoon breaks may have lasted for decades or even centuries, leading to intense drought periods on the Indian subcontinent. Precipitation proxy data from speleothems in Oman show a more gradual decrease in precipitation during the Holocene associated with a southward migration of the Inter-Tropical Convergence Zone (ITCZ) (Fleitmann et al. 2003), which parallels the decrease in summer monsoon winds reconstructed offshore Oman (Gupta et al. 2003).

6.2 Pleistocene Variability on Suborbital and Orbital Timescales

A recent high-resolution proxy record of chemical alteration and provenance from the Andaman Sea indicates that the chemical weathering in the Myanmar watersheds intensified during the deglacial to mid-Holocene summer monsoon intensification (Miriyala et al. 2017). Increased silicate weathering started with the deglacial warming at ~17.7 ka and intensified at ~15.5 ka with Northern Hemisphere warming during the Bølling-Allerød. These findings are in broad agreement with deglacial salinity reconstructions, based on oxygen isotopes combined with temperature estimates from surface, thermocline and bottom dwelling foraminifers in the Andaman Sea

along a latitudinal transect between 5 and 20° N (Gebregiorgis et al. 2016; Sijinkumar et al. 2016). These studies suggested that mid-Holocene (9–6 ka) mixed layer waters in the Andaman Sea were 3.8 PSU fresher than today, whereas they were essentially the same as today during the LGM, in contrast to the more saline water masses in the Bay of Bengal. Sijinkumar et al. (2016) explained the relative freshness of the Andaman Sea during the LGM through the lowered sea level, which reduced surface water interchange with the open Bay of Bengal and decreased the distance of the core locations to the river outflow. Surface- and thermocline-dwelling planktic foraminifers in the Andaman Sea and northern Bay of Bengal display increased $\delta^{18}O$ during the YD, indicating lower temperature and/or increased salinity linked to colder and dryer conditions in the hinterland due to weakened summer monsoon coupled with enhanced winter monsoon mixing of surface ocean water with deeper upper thermocline water. Interestingly, these suborbital changes in monsoonal intensity cannot be related to local insolation forcing, since Northern Hemisphere insolation consistently increased during the YD.

Orbital-scale mixed layer and thermocline temperatures and $\delta^{18}O$ records from the northern end of the Ninetyeast Ridge and Andaman Sea spanning the past 1 million years (Fig. 10) suggested that internal forcing mechanisms such as global ice volume and the temperature gradient between high and low latitudes exert major influence on the timing and spectral characteristics of monsoon precipitation proxies (Bolton et al.

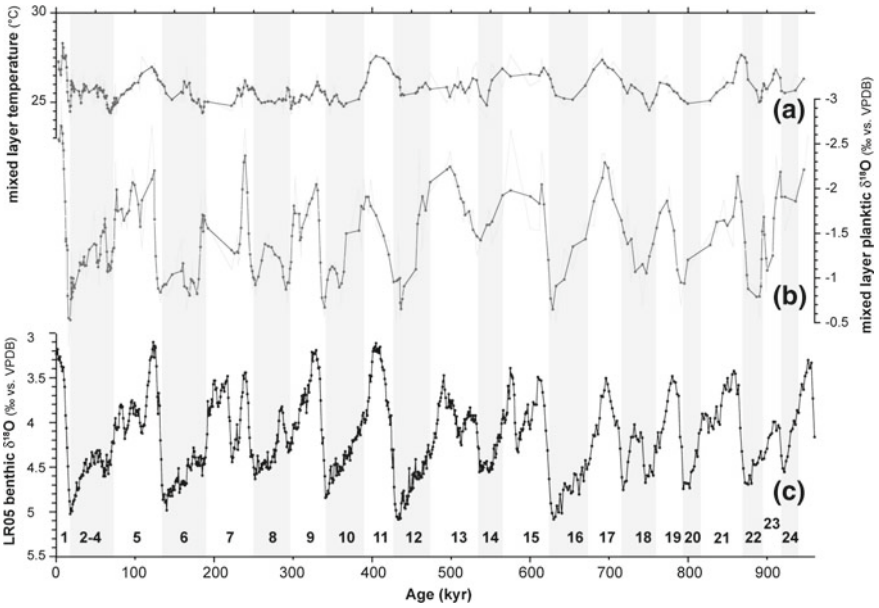

Fig. 10 Mg/Ca-derived mixed layer temperature at National Gas Hydrate Program (NGHP) Site 17 from Gebregiorgis et al. (2018) (**a**). Oxygen isotope ratios of the mixed-layer dwelling foraminifer *G. sacculifer* from Gebregiorgis et al. (2018) (**b**). Benthic oxygen isotope stack from Lisiecki and Raymo (2005) (**c**). Glacial stages are marked by gray shading

2013; Gebregiorgis et al. 2018). Spectral analyses of reconstructed seawater $\delta^{18}O$ time series indicated that upper water column stratification minima (corresponding to maxima in monsoonal wind strength) and Indian monsoon precipitation maxima lag Northern Hemisphere summer insolation maxima by ~9 kyr. This long time lag is at odds with a direct insolation forcing of the Indian summer monsoon in the Andaman Sea (Bolton et al. 2013; Gebregiorgis et al. 2018). However, precipitation maxima are in phase with obliquity minima, which coincide with intensified temperature gradients between the tropics and the Southern Hemisphere Indian Ocean, where the main moisture source for the Indian Monsoon is located (Ding et al. 2004; Clemens et al. 2008). This sensitivity of monsoonal precipitation in the Andaman area to Southern Hemisphere climate change suggests that the Indian Monsoon during the Pleistocene was mainly forced by internal processes, including changes in global ice volume and in the interhemispheric temperature gradient, rather than by direct insolation over the Asian landmass.

6.3 Late Miocene-Pliocene Evolution of the Indian Monsoon

The Miocene-Pliocene climate transition is characterized by a global cooling trend, which started at ~7.2 Ma and lasted until ~5.5 Ma (Herbert et al. 2016), culminating in two major high latitude cooling events (benthic $\delta^{18}O$ maxima TG14 and TG12) between 5.6 and 5.5 Ma (Holbourn et al. 2018). This cooling trend was followed by relatively rapid warming in the tropical northwestern Pacific Ocean between ~5.5 and ~5.3 Ma (Holbourn et al. 2018). These long-term climate fluctuations were associated with strengthening of the dry and cold East Asian winter monsoon between ~7.2 and ~5.5 Ma and intensification of the wet and warm summer monsoon between ~5.5 and ~5.3 Ma (Holbourn et al. 2018). The Andaman Sea Sites U1447 and U1448 recovered these intervals in unprecedented resolution (Fig. 9), allowing a first comparison of the response of the East Asian and Indian Monsoon subsystems to major episodes of global cooling and warming.

The lower part of Hole U1447A (Cores 68X to 88X, ~546.50–740.46 m drilled depth) provides insights into the evolution of the Indian Monsoon at a location directly influenced by the discharge of the Irrawaddy and Salween Rivers into the Andaman Sea (Fig. 11). Potassium (K) contents derived from spectral natural gamma ray (NGR) measurements in combination with shipboard biostratigraphy reveal a distinct change in sediment provenance and/or in climatic conditions and erosion in the sediment source area between ~7 and ~6 Ma. Spectral NGR logging allows to reliably estimate sedimentary contents of K from the characteristic gamma-ray energies of isotopes in the ^{40}K and ^{232}Th radioactive decay series by integrating counts over specific energy levels of the NGR spectrum (Dunlea et al. 2013; De Vleeschouwer et al. 2017). The elements Th and K are linked to the detrital clay fraction, in particular K commonly characterizes high illite content associated with dominant physical weathering and/or high erosion rates in the source area. Cross-plots of Th (ppm) versus K (%) are used in petrophysical log evaluation to discriminate between different clay types.

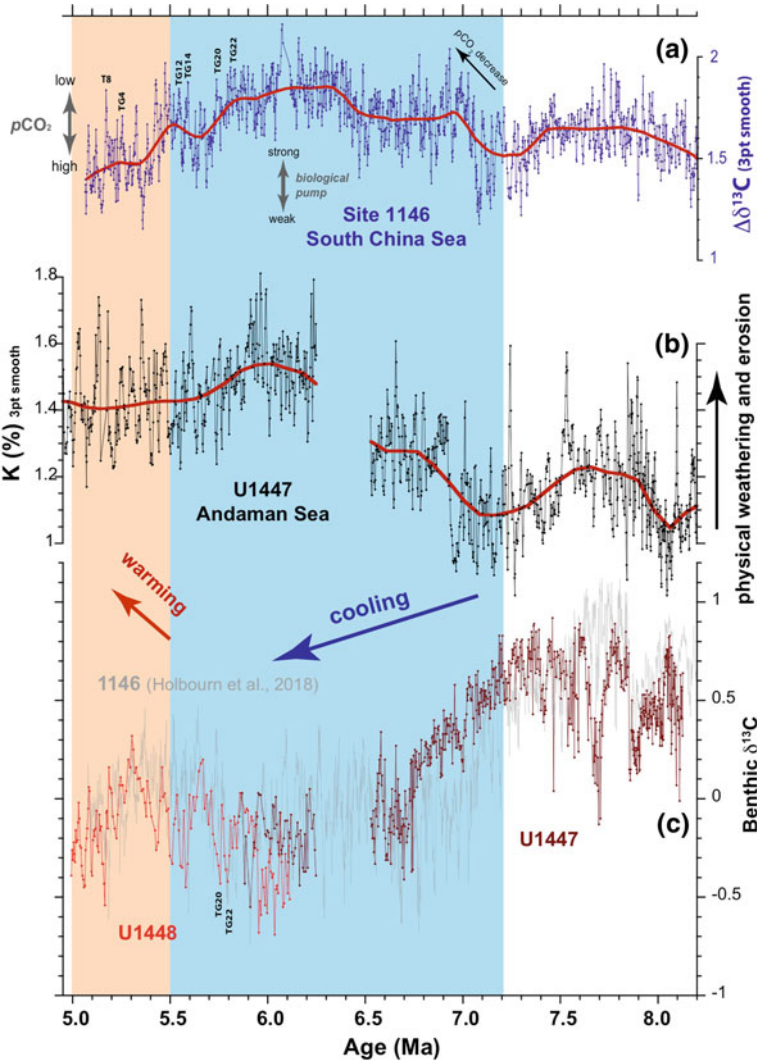

Fig. 11 Comparison of late Miocene (8.2–5 Ma) Indian and East Asian (South China Sea) Monsoon evolution. $\delta^{13}C$ gradient between mixed layer and epifaunal deep water benthic foraminifers at South China Sea ODP Site 1146 from Holbourn et al. (2018) (**a**), change in monsoonal terrigenous runoff (% K) derived from shipboard spectral gamma ray logging in Hole U1447A (**b**), and Sites U1447 and U1448 benthic foraminiferal $\delta^{13}C$ records from the Andaman Sea (**c**). Age models of Sites U1447 and U1448 are derived through correlation with ODP Sites 982 and 1146 orbitally-tuned benthic $\delta^{13}C$ records (Drury et al. 2018; Holbourn et al. 2018—gray background curve). Red smooth curves in (**a**) and (**b**) are fitted using the locally weighted least squared error (LOWESS) method

Generally, a Th/K ratio of >12 is suggested for kaolinitic clays and a Th/K ratio of >2 for illite (Schlumberger Crossplots for Porosity, Lithology and Saturation, CP19 Mineral Identification from NGS* Natural Gamma Ray Spectrometry Log).

In Hole U1447A, the change from K-depleted sediment discharge (indicating dominant chemical weathering in the source area) to K-enriched, illite-dominated discharge (from areas with prevalent physical weathering) coincides with the onset of global cooling at ~7.2 Ma (Fig. 11). The changes in the chemical composition of terrigenous runoff towards more K-rich sediments between ~7.1 and ~6.8 Ma and between ~6.5 and ~6.2 Ma may also relate to changes in erosional patterns in the sediment source area due to the onset of more seasonal monsoonal rainfall. Similar changes occur in the runoff of the Brahmaputra and Ganges Rivers towards the Bay of Bengal, where K-enriched, illite dominated terrigenous runoff is associated with increased erosion of physically weathered sediments during Pleistocene phases of strong monsoonal seasonality (Derry and France-Lanord 1997; Colin et al. 2006).

The long-term late Miocene cooling trend was also punctuated by transient Northern Hemisphere cooling events (TG isotope stages of Shackleton et al. 1995) between 6.5 and 5.5 Ma (Holbourn et al. 2018). These TG cold stages are strongly imprinted on the Andaman Sea mixed layer and intermediate water $\delta^{18}O$ (Fig. 12) and on the mixed layer Mg/Ca records. However, the amplitude of glacial-interglacial differences was substantially higher during the Pleistocene (~1.4‰ for MIS10 and MIS 11 compared to ~0.9‰ for TG21 and TG20), which likely reflects differences in Northern Hemisphere ice volume and hydrologic regimes over Asian mountain ranges during more extreme Pleistocene glacial conditions. The ~1‰ $\delta^{18}O$ difference between modern and late Miocene warm stages can only partly be explained by warmer mixed layer temperatures during the warmer Miocene, but also includes a component of increased monsoonal runoff and precipitation during periods of warmer climate.

7 Conclusions and Outlook

Climate models in combination with instrumental observations predict that over the next few centuries, global warming may significantly increase the spatial heterogeneity of monsoonal precipitation (Ashfaq et al. 2009; Loo et al. 2015). These model simulations suggest that enhanced greenhouse forcing results in suppression of summer precipitation and a delay in the onset of the Indian Monsoon over large (northern) parts of the Indian subcontinent and the Bay of Bengal, whereas the Andaman Sea and its Indo-Burman hinterland will receive enhanced precipitation (Ashfaq et al. 2009). The spliced sediment archive of Sites U1447 and U1448, recently drilled during IODP Expedition 353 (iMonsoon), will provide the first complete millennial-scale resolution mixed layer temperature and salinity records over the late Neogene in one of the core areas of the Indian Monsoon. Ongoing research on the sediment successions recovered by this expedition and other recent IODP Expeditions in the Indian Ocean and western Pacific marginal seas will improve understanding of the

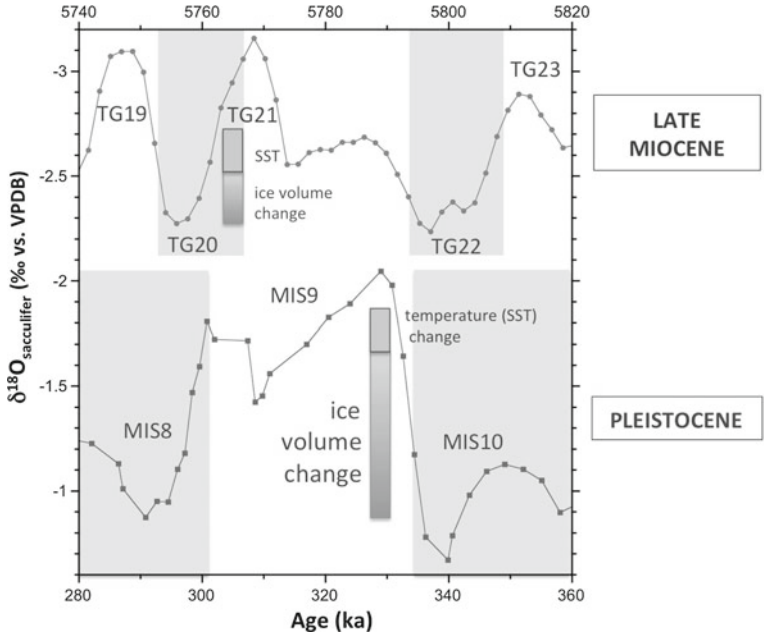

Fig. 12 Comparison of mixed layer (*Trilobatus sacculifer)* $\delta^{18}O$ across late Miocene TG Events 20 and 22 at Site U1448 (3 point moving average) and across Pleistocene MIS 9–13 at NGHP 17 (3 point moving average $\delta^{18}O$ data from Gebregiorgis et al. 2018). Change in Mg/Ca derived mixed layer temperature is based on Jöhnck et al. (unpublished data) for the late Miocene and on Gebregiorgis et al. (2018) for the Pleistocene. Ice volume change was estimated as 50 and 70% of benthic $\delta^{18}O$ variability for the late Miocene and Pleistocene, respectively. Glacial stages are shaded gray

primary forcing mechanisms on regional monsoonal subsystems and help constrain projections of future trends on a warmer Earth.

Acknowledgements This research used data and samples provided by the International Ocean Discovery Program (IODP). We are grateful to the IODP Expedition 353 shipboard party for all their efforts. Funding for this research was provided by the German Research Foundation (DFG) priority program (SPP) 527, grant KU649/35-1. We thank David De Vleeshouwer for making available potassium percentages from IODP Expedition 353 shipboard spectral natural gamma ray data and two anonymous reviewers for corrections and helpful suggestions to improve this manuscript.

References

Al Azhar M, Lachkar Z, Lévy M, Smith S (2017) Oxygen minimum zone contrasts between the Arabian Sea and the Bay of Bengal implied by differences in remineralization depth. Geophys Res Lett 44(21):11–106, 114. https://doi.org/10.1002/2017GL075157

Ali S, Hathorne EC, Frank M, Gebregiorgis D, Stattegger K, Stumpf R, Kutterolf S, Johnson JE, Giosan L (2015) South Asian monsoon history over the past 60 kyr recorded by radiogenic isotopes and clay mineral assemblages in the Andaman Sea. Geochem Geophys Geosyst 16(2):505–521. https://doi.org/10.1002/2014GC005586

Allen R, Carter A, Najman Y, Bandopadhya PC, Chapman HJ, Bickle J, Garzanti E, Vezzoli G, Andò S, Foster GL, and Gerring C (2008) New constraints on the sedimentation and uplift history of the Andaman-Nicobar accretionary prism, South Andaman Island. In: Draut A, Clift PD, Scholl DW (eds) Formation and applications of the sedimentary record in Arc Collision Zones, vol 436, pp 223–255. Geological Society of America Special Papers. https://doi.org/10.1130/2007.2436(11)

An ZS, Kutzbach JE, Prell WL, Porter SC (2001) Evolution of Asian monsoons and phased uplift of the Himalaya-Tibetan Plateau since Late Miocene times. Nature 411:62–66. https://doi.org/10.1038/35075035

An Z, Wu G, Li J, Sun Y, Liu Y, Zhou W, Cai Y, Duan A, Li L, Mao J, Cheng H, Shi Z, Tan L, Yan H, Ao H, Chang H, Feng J (2015) Global monsoon dynamics and climate change. Annu Rev Earth Planet Sci 43:29–77. https://doi.org/10.1146/annurev-earth-060313-054623

Ashfaq M, Shi Y, Tung W-W, Trapp RJ, Gao X, Pal JS, Diffenbaugh NS (2009) Suppression of south Asian summer monsoon precipitation in the 21st century. Geophys Res Lett 36:L01704. https://doi.org/10.1029/2008GL036500

Aung LL, Zin EE, Theingi P, Elvera N, Aung PP, Han TT, Oo Y, Skaland RG (2017) Myanmar climate report, MET report. Norwegian Meteorological Institute, Sept 2017, p 105

Awasthi N, Ray JS, Singh AK, Band ST, Rai VK (2014) Provenance of the Late Quaternary sediments in the Andaman Sea: implications for monsoon variability and ocean circulation. Geochem Geophys Geosyst 15(10):3890–3906. https://doi.org/10.1002/2014GC005462

Bhattacharjee D (2005) Pteropod preservation profiles in seabed sediments off Middle Andaman Island in Andaman Sea. Indian J Mar Sci 34(3):259–266. http://nopr.niscair.res.in/handle/123456789/1561

Bolton CT, Chang L, Clemens SC, Kodama K, Ikehara M, Medina-Elizalde M, Paterson GA, Roberts AP, Rohling EJ, Yamamoto Y, Zhao X (2013) A 500,000 year record of Indian summer monsoon dynamics recorded by eastern equatorial Indian Ocean upper water-column structure. Quat Sci Rev 77:167–180. https://doi.org/10.1016/j.quascirev.2013.07.031

Boos WR, Kuang Z (2010) Dominant control of the South Asian monsoon by orographic insulation versus plateau heating. Nature 463(7278):218–223. https://doi.org/10.1038/nature08707

Brewer D, Hayes D, Lyne V, Donovan A, Skewes T, Milton D, Murphy N (2015) An ecosystem characterisation of the Bay of Bengal. Bay of Bengal Large Marine Ecosystem Project, BOBLME-2015-Ecology-13

Cao P, Shi X, Li W, Liu S, Yao Z, Hu L, Khokiattiwong S, Kornkanitnan N (2015) Sedimentary responses to the Indian Summer Monsoon variations recorded in the southeastern Andaman Sea slope since 26 ka. J Asian Earth Sci 114:512–525. https://doi.org/10.1016/j.jseaes.2015.06.028

Cawthern T, Johnson JE, Giosan L, Flores JA, Rose K, Solomon E (2014) A late Miocene-early Pliocene biogenic silica crash in the Andaman Sea and Bay of Bengal. Mar Petroleum Geol 58:490–501. https://doi.org/10.1016/j.marpetgeo.2014.07.026

Cerling TE, Harris JM, MacFadden BJ, Leakey MG, Quade J, Eisenmann V, Ehleringer JR (1997) Global vegetation change through the Miocene/Pliocene boundary. Nature 389(6647):153–158. https://doi.org/10.1038/38229

Chatterjee A, Shankar D, McCreary JP, Vinayachandran PN, Mukherjee A (2017) Dynamics of Andaman Sea circulation and its role in connecting the equatorial Indian Ocean to the Bay of Bengal. J Geophys Res Oceans 122(4):3200–3218. https://doi.org/10.1002/2016JC012300

Clemens SC, Prell WL (2007) The timing of orbital scale Indian-monsoon changes. Quat Sci Rev 26(3–4):275–278. https://doi.org/10.1016/j.quascirev.2006.11.010

Clemens SC, Kuhnt W, LeVay LJ and the Expedition 353 Scientists (2016) Indian monsoon rainfall. In: Proceedings of the international Ocean discovery program 353, College Station, TX. http://dx.doi.org/10.14379/iodp.proc.353.108.2016

Clemens SC, Prell WL, Sun Y, Liu Z, Chen G (2008) Southern Hemisphere forcing of Pliocene δ18O and the evolution of Indo-Asian monsoons. Paleoceanography 23:PA4210. https://doi.org/10.1029/2008pa001638

Clift PD, Plumb RA (2008) The Asian Monsoon: causes, history and effects. Cambridge University Press, p 288. ISBN 978-0-521-84799-5

Clift PD, Hodges KV, Heslop D, Hannigan R, Van Long H, Calves G (2008) Correlation of Himalayan exhumation rates and Asian monsoon intensity. Nat Geosci 1(12):875–880. https://doi.org/10.1038/ngeo351

Colin C, Turpin L, Bertaux J, Desorairies A, Kissel C (1999) Erosional history of the Himalayan and Burman ranges during the last two glacial–interglacial cycles. Earth Planet Sci Lett 171(4):647–660. https://doi.org/10.1016/S0012-821X(99)00184-3

Colin C, Turpin L, Blamart D, Frank N, Kissel C, Duchamp S (2006) Evolution of weathering patterns in the Indo-Burman ranges over the last 280 kyr: effects of sediment provenance on 87Sr/86Sr ratios tracer. Geochem Geophys Geosyst 7(3):Q03007. https://doi.org/10.1029/2005GC000962

Curray JR (2005) Tectonics and history of the Andaman Sea region. J Asian Earth Sci 25:187–232. https://doi.org/10.1016/j.jseaes.2004.09.001

Day J, Fung I, Risi C (2015) Coupling of South and East Asian monsoon precipitation in July–August. J Clim 28(11):4330–4356. https://doi.org/10.1175/JCLI-D-14-00393.1

De Vleeschouwer D, Dunlea AG, Auer G, Anderson CH, Brumsack H, de Loach A, Gurnis M, Huh Y, Ishiwa T, Jang K, Kominz MA, März C, Schnetger B, Murra RW, Pälike H, and Expedition 356 Shipboard Scientists (2017) Quantifying K, U, and Th contents of marine sediments using shipboard natural gamma radiation spectra measured on DV JOIDES Resolution. Geochem Geophys Geosyst 18(3):1053–1064. https://doi.org/10.1002/2016GC006715

Derry LA, France-Lanord C (1997) Himalayan weathering and erosion fluxes: climate and tectonic controls. In: Ruddiman WF (eds) Tectonic uplift and climate change. Plenum Press, New York. https://doi.org/10.1007/978-1-4615-5935-1-12

Ding Y et al (2004) Overview of the South China Sea monsoon experiment. Adv Atmos Sci 21:343–360. https://doi.org/10.1007/BF02915563

Drury AJ, Westerhold T, Hodell D, Röhl U (2018) Reinforcing the North Atlantic backbone: revision and extension of the composite splice at ODP Site 982. Clim Past 14:321–338. https://doi.org/10.5194/cp-14-321-2018

Dunlea AG, Murray RW, Harris RN, Vasiliev MA, Evans H, Spivack AJ, D'Hondt S (2013) Assessment and use of NGR instrumentation on the JOIDES Resolution to quantify U, Th, and K concentrations in marine sediment. Sci Drill 15:57–63. https://doi.org/10.2204/iodp.sd.15.05.2013

Fleitmann D, Burns SJ, Neff U, Mangini A, Matter A (2003) Changing moisture sources over the last 330,000 years in Northern Oman from fluid-inclusion evidence in speleothems. Quat Res 60(2):223–232. https://doi.org/10.1016/S0033-5894(03)00086-3

France-Lanord C, Derry L, Michard A (1993) Evolution of the Himalayas since Miocene time—isotopic and sedimentological evidence from the Bengal Fan. In: Treloar PJ, Searle MP (eds) Himalayan tectonics, vol 74, pp 603–621. Geological Society Special Publications. https://doi.org/10.1144/GSL.SP.1993.074.01.40

Frerichs WE (1971) Planktonic foraminifera in the sediments of the Andaman Sea. J Foramin Res 1(1):1–14. https://doi.org/10.2113/gsjfr.1.1.1

Gadgil S (2003) The Indian monsoon and its variability. Annu Rev Earth Planet Sci 31(1):429–467. https://doi.org/10.1146/annurev.earth.31.100901.141251

Garzanti E, Limonta M, Resentini A, Bandopadhyay PC, Najman Y, Andò S, Vezzoli G (2013) Sediment recycling at convergent plate margins (Indo-Burman Ranges and Andaman-Nicobar Ridge). Earth Sci Rev 123:113–132. https://doi.org/10.1016/j.earscirev.2013.04.008

Gauns M, Madhupratap M, Ramaiah N, Jyothibabu R, Fernandes V, Paul JT, Prasanna Kumar S (2005) Comparative accounts of biological productivity characteristics and estimates of carbon fluxes in the Arabian Sea and the Bay of Bengal. Deep Sea Res Part 2 Top Stud Oceanogr 52(14–15):2003–2017. https://doi.org/10.1016/j.dsr2.2005.05.009

Gebregiorgis D, Hathorne EC, Sijinkumar AV, Nagender Nath B, Nürnberg D, Frank M (2016) South Asian summer monsoon variability during the last ~54 kyrs inferred from surface water salinity and river run off proxies. Quat Sci Rev 138:6–15. https://doi.org/10.1016/j.quascirev.2016.02.012

Gebregiorgis D, Hathorne EC, Giosan L, Clemens S, Nürnberg D, Frank M (2018) Southern Hemisphere forcing of South Asian monsoon precipitation over the past ~1 million years. Nat Commun 9(1):4702. https://doi.org/10.1038/s41467-018-07076-2

Gordon AL, Shroyer EL, Mahadevan A, Sengupta D, Freilich M (2016) Bay of Bengal: 2013 northeast monsoon upper-ocean circulation. Oceanography 29(2):82–91. https://doi.org/10.5670/oceanog.2016.41

Goswami BN, Rao SA, Sengupta D, Chakravorty S (2016) Monsoons to mixing in the Bay of Bengal: Multiscale air-sea interactions and monsoon predictability. Oceanography 29(2):18–27. https://doi.org/10.5670/oceanog.2016.35

Guo ZT, Ruddiman WF, Hao QZ, Wu HB, Qiao YS, Zhu RX, Peng SZ, Wei JJ, Yuan BY, Liu TS (2002) Onset of Asian desertification by 22 Myr ago inferred from loess deposits in China. Nature 416(6877):159–163. https://doi.org/10.1038/416159a

Gupta AK, Anderson DM, Overpeck JT (2003) Abrupt changes in the Asian southwest monsoon during the Holocene and their links to the North Atlantic Ocean. Nature 421(6921):354–357. https://doi.org/10.1038/nature01340

Haq BU, Hardenbol JAN, Vail PR (1987) Chronology of fluctuating sea levels since the Triassic. Science 235(4793):1156–1167. https://doi.org/10.1126/science.235.4793.1156

Harrison TM, Copeland P, Kidd WSF, Yin AN (1992) Raising Tibet. Science 255(5052):1663–1670. https://doi.org/10.1126/science.255.5052.1663

Hastenrath S, Lamb PJ (1979) Climatic Atlas of the Indian Ocean, Part I, Surface climate and atmospheric circulation. University of Wisconsin Press, Madison, p 116. ISBN 0299078140 9780299078140

Herbert TD, Lawrence KT, Tzanova A, Peterson LC, Caballero-Gill R, Kelly CS (2016) Late Miocene global cooling and the rise of modern ecosystems. Nat Geosci 9(11):843–847. https://doi.org/10.1038/ngeo2813

Holbourn AE, Kuhnt W, Schulz M, Erlenkeuser H (2005) Impacts of orbital forcing and atmospheric carbon dioxide on Miocene ice-sheet expansion. Nature 438(7067):483–487. https://doi.org/10.1038/nature04123

Holbourn AE, Kuhnt W, Schulz M, Flores J-A, Andersen N (2007) Orbitally-paced climate evolution during the middle Miocene "Monterey" carbon isotope excursion. Earth Planet Sci Lett 261(3–4):534–550. https://doi.org/10.1016/j.epsl.2007.07.026

Holbourn AE, Kuhnt W, Clemens SC, Kochhann KDG, Jöhnck J, Lübbers J, Andersen N (2018) Late Miocene climate cooling and intensification of southeast Asian winter monsoon. Nat Commun 9(1):1584. https://doi.org/10.1038/s41467-018-03950-1

Huang Y, Clemens SC, Liu W, Wang Y, Prell WL (2007) Large-scale hydrological change drove the late Miocene C4 plant expansion in the Himalayan foreland and Arabian Peninsula. Geology 35(6):531–534. https://doi.org/10.1130/G23666A.1

Ittekkot V, Nair RR, Honjo S, Ramaswamy V, Bartsch M, Manganini S, Desai BN (1991) Enhanced particle fluxes in Bay of Bengal induced by injection of fresh water. Nature 351(6325):385–387. https://doi.org/10.1038/351385a0

Iversen MH, Ploug H (2010) Ballast minerals and the sinking carbon flux in the ocean: Carbon-specific respiration rates and sinking velocity of marine snow aggregates. Biogeosciences 7(9):2613–2624. https://doi.org/10.5194/bg-7-2613-2010

Klaas C, Archer DE (2002) Association of sinking organic matter with various types of mineral ballast in the deep sea: implications for the rain ratio. Glob Biogeochem Cycles 16(4):1116. https://doi.org/10.1029/2001GB001765

Kroon D, Steens T, Troelstra SR (1991) Onset of monsoonal related upwelling in the western Arabian Se as revealed by planktonic foraminifers. In: Prell WL, Niitsuma N et al (eds) Proceedings of the

Ocean drilling program, scientific results, vol 117. College Station, TX (Ocean Drilling Program), pp 257–263. http://dx.doi.org/10.2973/odp.proc.sr.117.126.1991
Kwon EY, Primeau F, Sarmiento JL (2009) The impact of remineralization depth on the air–sea carbon balance. Nat Geosci 2(9):630–635. https://doi.org/10.1038/ngeo612
Le Moigne FAC, Gallinari M, Laurenceau E, De La Rocha CL (2013) Enhanced rates of particulate organic matter remineralization by microzooplankton are diminished by added ballast minerals. Biogeosciences 10(9):5755–5765. https://doi.org/10.5194/bg-10-5755-2013
Lisiecki LE, Raymo ME (2005) A Pliocene—Pleistocene stack of 57 globally distributed benthic δ18O records. Paleoceanography 20(1):PA1003. https://doi.org/10.1029/2004PA001071
Liu X, Yin Z (2011) Forms of the Tibetan Plateau uplift and regional differences of the Asian monsoon-arid environmental evolution—a modeling perspective. Earth Environ 2(3):401–416
Liu J, Wang B, Yang J (2008) Forced and internal modes of variability of the East Asian summer monsoon. Clim Past 4:225–233. www.clim-past.net/4/225/2008/
Loo YY, Billa L, Singh A (2015) Effect of climate change on seasonal monsoon in Asia and its impact on the variability of monsoon rainfall in Southeast Asia. Geosci Front 6:817–823. https://doi.org/10.1016/j.gsf.2014.02.009
Lutz M, Dunbar R, Caldeira K (2002) Regional variability in the vertical flux of particulate organic carbon in the ocean interior. Global Biogeochem Cycles 16(3):1037. https://doi.org/10.1029/2000GB001383
Milliman JD, Farnsworth KL (2011) River discharge to the Coastal Ocean. Cambridge University Press, p 384. ISBN 978-0-521-87987-3
Miriyala P, Sukumaran NP, Nath BN, Ramamurty PB, Sijinkumar AV, Vijayagopal B, Ramaswamy V, Tyson S (2017) Increased chemical weathering during the deglacial to mid-Holocene summer monsoon intensification. Sci Rep 7:44310. https://doi.org/10.1038/srep44310
Molnar P (2005) Mio–Pliocene growth of the Tibetan Plateau and evolution of East Asian climate. Palaeontol Electron 8(1):1–23. http://palaeo-electronica.org/2005_1/molnar2/molnar2.pdf
Molnar P, Rajagopalan B (2012) Late Miocene upward and outward growth of eastern Tibet and decreasing monsoon rainfall over the northwestern Indian subcontinent since ~10 Ma. Geophys Res Lett 39(9):L09702. https://doi.org/10.1029/2012GL051305
Molnar P, England P, Martinod J (1993) Mantle dynamics, uplift of the Tibetan Plateau, and the Indian Monsoon. Rev Geophys 31(4):357–396. https://doi.org/10.1029/93RG02030
Molnar P, Boos WR, Battisti DS (2010) Orographic controls on climate and paleoclimate of Asia: thermal and mechanical roles for the Tibetan Plateau. Annu Rev Earth Planet Sci 38(1):77–102. https://doi.org/10.1146/annurev-earth-040809-152456
Morley CK (2016) Cenozoic structural evolution of the Andaman Sea: evolution from an extensional to a sheared margin. In: Nemcok M, Rybar S, Sinha ST, Hermeston SA, Ledvenyiova L (eds) Transform margins: development, controls and petroleum systems, vol 431. Geological Society Special Publications, pp 39–61. http://doi.org/10.1144/SP431.1
Pandey DK, Anitha G, Prerna R, Pandey A (2017) Late Cenozoic seismic stratigraphy of the Andaman Forearc Basin, Indian Ocean. Pet Sci 14(4):648–661. https://doi.org/10.1007/s12182-017-0197-7
Phillips SC, Johnson JE, Underwood MB, Guo J, Giosan L, Rose K (2014) Long-timescale variation in bulk and clay mineral composition of Indian continental margin sediments in the Bay of Bengal, Arabian Sea, and Andaman Sea. Mar Petroleum Geol 58:117–138. https://doi.org/10.1016/j.marpetgeo.2014.06.018
Ponton C, Giosan L, Eglinton TI, Fuller DQ, Johnson JE, Kumar P, Collett TS (2012) Holocene aridification of India. Geophys Res Lett 39(3):L03704. https://doi.org/10.1029/2011GL050722
Prell WL, Kutzbach JE (1997) The Impact of Tibet-Himalayan elevation on the sensitivity of the monsoon climate system to changes in solar radiation. In: Ruddiman WJ (ed) Tectonic uplift and climate change. Plenum Press, New York, pp 171–201. https://doi.org/10.1007/978-1-4615-5935-1
Prell WL, Murray DW, Clemens SC, Anderson DM (1992) Evolution and variability of the Indian Ocean summer monsoon: evidence from the western Arabian Sea drilling program. In: Duncan

RA, Rea DK, Kidd RB, Rad U, Weissel JK (eds) Synthesis of results from scientific drilling in the Indian Ocean, vol 70. Geophysical Monograph, pp 447–469. http://dx.doi.org/10.1029/GM070p0447

Qiu J (2013) Monsoon Melee. Science 340(6139):1400–1401. https://doi.org/10.1126/science.340.6139.1400

Quade J, Cerling TE (1995) Expansion of C4 grasses in the late Miocene of northern Pakistan: evidence from stable isotopes in paleosols. Palaeogeogr Palaeoclimatol Palaeoecol 115(1–4):91–116. https://doi.org/10.1016/0031-0182(94)00108-K

Raju KAK, Ramprasad T, Rao PS, Ramalingeswara Rao BR, Varghese J (2004) New insights into the tectonic evolution of the Andaman basin, northeast Indian Ocean. Earth Planet Sci Lett 221:145–162. https://doi.org/10.1016/S0012-821X(04)00075-5

Ramaswamy V, Rao PS, Rao KH, Thwin S, Srinavasa Rao N, Raiker V (2004) Tidal influence on suspended sediment distribution and dispersal in the northern Andaman Sea and Gulf of Martaban. Mar Geol 208(1):33–42. https://doi.org/10.1016/j.margeo.2004.04.019

Rodriguez M, Chamot-Rooke N, Huchon P, Fournier M, Delescluse M (2014) The Owen Ridge uplift in the Arabian Sea: implications for the sedimentary record of Indian monsoon in late Miocene. Earth Planet Sci Lett 394:1–12. https://doi.org/10.1016/j.epsl.2014.03.011

Ruddiman WF (2006) What is the timing of orbital-scale monsoon changes? Quat Sci Rev 25(7):657–658. https://doi.org/10.1016/j.quascirev.2006.02.004

Sandwell DT, Smith WHF (2009) Global marine gravity from retracked Geosat and ERS 1 altimetry: ridge segmentation v. spreading rate. J Geophys Res 114:B01411. https://doi.org/10.1029/2008jb006008

Sarkar A, Ramesh R, Somayajulu BLK, Agnihotri R, Jull AJT, Burr GS (2000) High resolution Holocene monsoon record from the eastern Arabian Sea. Earth Planet Sci Lett 177(3–4):209–218. https://doi.org/10.1016/S0012-821X(00)00053-4

Schott FA, Xie S-P, McCreary JP Jr (2009) Indian Ocean circulation and climate variability. Rev Geophys 47:RG1002. http://dx.doi.org/10.1029/2007RG000245

Shackleton NJ, Hall MA, Pate D (1995) Pliocene stable isotope stratigraphy of Site 846. In: Pisias NG, Mayer LA, Janecek TR, Palmer-Julson A, van Andel TH (eds) Proceedings of ODP, scientific results, vol 138. College Station, TX (Ocean Drilling Program), pp 337–355. https://doi.org/10.2973/odp.proc.sr.138.117.1995

Sijinkumar A, Clemens S, Nath BN, Prell W, Benshila R, Lengaigne M (2016) $\delta^{18}O$ and salinity variability from the last glacial maximum to recent in the Bay of Bengal and Andaman Sea. Quat Sci Rev 135:79–91. https://doi.org/10.1016/j.quascirev.2016.01.022

Singh SC, Moeremans R, McArdle J, Johansen K (2013) Seismic images of the silver strike-slip fault and back thrust in the Andaman-Nicobar region. J Geophys Res 118:5208–5224. https://doi.org/10.1002/jgrb.50378

Sinha A, Berkelhammer M, Stott L, Mudelsee M, Cheng H, Biswas J (2011a) The leading mode of Indian summer monsoon precipitation variability during the last millennium. Geophys Res Lett 38:L15703. https://doi.org/10.1029/2011GL047713

Sinha A, Stott L, Berkelhammer M, Cheng H, Edwards RL, Buckley B, Aldenderfer M, Mudelsee M (2011b) A global context for megadroughts in monsoon Asia during the past millennium. Quat Sci Rev 30:47–62. https://doi.org/10.1016/j.quascirev.2010.10.005

Staubwasser M, Weiss H (2006) Holocene climate and cultural evolution in late prehistoric-early historic west Asia—Introduction. Quat Res 66(3):372–387. https://doi.org/10.1016/j.yqres.2006.09.001

Sun X, Wang P (2005) How old is the Asian monsoon system?—Palaeobotanical records from China. Palaeogeogr Palaeoclimatol Palaeoecol 222(3–4):181–222. https://doi.org/10.1016/j.palaeo.2005.03.005

Talley LD (2013) Hydrographic atlas of the world Ocean circulation experiment (WOCE), vol 4. Indian Ocean. ISBN: 0904175588

Tomczak M, Godfrey JS (2005) Regional Oceanography: an introduction, pdf version 1.1. Chapter 12, hydrology of the Indian Ocean, pp 199–214. http://www.incois.gov.in/Tutor/regoc/pdfversion.html

Unger D, Jennerjahn T (2009) Impact of regional Indian Ocean characteristics on the biogeochemical variability of settling particles. American Geophysical Union Geophysical Monograph Series, vol 185, pp 257-280. https://doi.org/10.1029/2008GM000703

Unger D, Ittekkot V, Schäfer P, Tiemann J, Reschke S (2003) Seasonality and interannual variability of particle fluxes to the deep Bay of Bengal: influence of riverine input and oceanographic processes. Deep Sea Res Part 2 Top Stud Oceanogr 50(5):897–923. https://doi.org/10.1016/S0967-0645(02)00612-4

Varkey MJ, Murty VSN, Suryanarayana A (1996) Physical oceanography of the Bay of Bengal and Andaman Sea. Oceanogr Mar Biol 34:1–70

Wan SM, Li AC, Clift PD, Stutt JB (2007) Development of the East Asian monsoon: mineralogical and sedimentologic records in the northern South China Sea since 20 Ma. Palaeogeogr Palaeoclimatol Palaeoecol 254(3–4):561–582. https://doi.org/10.1016/j.palaeo.2007.07.009

Wan S, Kürschner WM, Clift PD, Li A, Li T (2009) Extreme weathering/erosion during the Miocene Climatic Optimum: evidence from sediment record in the South China Sea. Geophys Res Lett 36:L19706. https://doi.org/10.1029/2009GL040279

Wang B, Ding QH (2008) Global monsoon: dominant mode of annual variation in the tropics. Dyn Atmos Oceans 44(3–4):165–183. https://doi.org/10.1016/j.dynatmoce.2007.05.002

Wang PX, Wang B, Cheng H, Fasullo J, Guo ZT, Kiefer T, Liu ZY (2017) The global monsoon across time scales: mechanisms and outstanding issues. Earth Sci Rev 174:84–121. https://doi.org/10.1016/j.earscirev.2017.07.006